RESEARCH PROJECTS IN THE ZHANG LAB

WASHINGTON STATE UNIVERSITY

INTRODUCTION

The Zhang group focuses on the development and application of multi-functional materials. There are three ongoing projects: 1) The design and development of luminescent Metal–Organic Frameworks (MOFs) for sensing; 2) The development of low-cost synthetic method for the production of hierarchically porous materials for catalysis; 3) Single-atom Catalysis.

RECENT PUBLICATIONS

1. "Energetic Systematics of Metal–Organic Frameworks: A Case Study of Al(III)-Trimesate MOF Isomers" Jiahong Li, Vitaliy G. Goncharov, Andrew C. Strzelecki, Hongwu Xu, Xiaofeng Guo*, and Qiang Zhang* Inorg. Chem. 2022, 61, 38, 15152–15165.
2. "MOF-Enabled Ion-Regulating Gel Electrolyte for Long-Cycling Lithium Metal Batteries Under High Voltage" Fu, Xuewei, Hurlock, Matthew J. , Ding, Chenfeng, Li, Xiaoyu, Zhang, Qiang,* Zhong, Wei-Hong*, Small, 2021, 2106225.
3. "Selective hydroxylation of aryl iodides to produce phenols under mild conditions using a supported copper catalyst" Leiduan Hao, Anika Auni, Guodong Ding, * Xiaoyu Li, Haiping Xu,Tao Li * and Qiang Zhang *, RSC Adv., 2021,11, 25348-25353
4. "Evolution of 14-Connected Zr_6 Secondary Building Units through Postsynthetic Linker Incorporation" Matthew J. Hurlock, Leiduan Hao, Kyle W. Kriegsman, Xiaofeng Guo, Michael O'Keeffe,* and Qiang Zhang* ACS Appl. Mater. Interfaces, 2021, 13, 44, 51945-51953. (Invited manuscript)
5. "Solvent-Free and Phase-Selective Synthesis of Aluminum Trimesate Metal–Organic Frameworks" Jiahong li, Matthew J. Hurlock, Vitaliy G. Goncharov, Xiaofeng Guo and Qiang Zhang*, Inorg. Chem. 2021, 60, 7, 4623-4632.
6. "Two Cd-Based Luminescent Coordination Polymers Constructed from a Truncated Linker" Matthew J. Hurlock, Monipak F. Lare, and Qiang Zhang*, Inorg. Chem. 2021, 60, 4, 2503–2513.
7. "Zr-based MOFs for oxidative desulfurization: What matters?" Leiduan Hao, Sebastian A Stoian Lydia, R. Weddle and Qiang Zhang*, Green Chem., 2020, 22, 6351-6356.
8. "Microwave-assisted Synthesis of Zirconium Phosphate Nanoplatelets Supported Ru-Anadem Nano-structures and Their Catalytic Study for the Hydrogenation of Acetophenone" Li, Xiaoyu; Ding, Guodong; Thompson, Brena; Hao, Leiduan; Deming, Derek; Heiden, Zachariah; Zhang, Qiang* ACS Appl. Mater. Interfaces. 2020, 12, 27, 30670–30679.
9. "Atomically dispersed palladium catalyses Suzuki–Miyaura reactions under phosphine-free conditions" Guodong Ding, Leiduan Hao, Haiping Xu, Liguang Wang, Jian Chen, Tao Li* & Qiang Zhang*, Comm. Chem., 2020, 3, Article number: 43.
10. "Metal–Organic Frameworks Towards Desulfurization of Fuels" Hao, L.; Hurlock, M. J.; Ding, G. Zhang, Q.* Topics Curr. Chem. 2020, 378:17
11. "A facile method to introduce iron secondary metal centers into metal–organic frameworks" Derek A. Deming, Matthew J. Hurlock, Xiaoyu Li, Kyle W. Kriegsman, Guodong Ding,Xiaofeng Guo, Qiang Zhang, J. Organomet. Chem. 2019, 897, 114-119.
12. "Efficient Oxidative Desulfurization Using a Mesoporous Zr-based MOF" Leiduan Hao, Matthew J. Hurlock, Xiaoyu Li, Guodong Ding, Kyle W. Kriegsman, Xiaofeng Guo, Qiang Zhang, Catal. Today, 2020, 350, 64-70.
13. "Hierarchically porous UiO-66: Facile synthesis, characterization and application" Leiduan Hao, Xiaoyu Li, Matthew J. Hurlock, Xin-Man Tu and Qiang Zhang Chem. Comm. 2018, 54, 11817-11820.
14. "Molecular Association Induced Emission Shifts for E/Z Isomers and Selective Sensing of Nitroaromatic Explosives" Matthew J. Hurlock, Yuwei Kan, Thibaut Lécrivain, Joseph L. Lapka, Kenneth L. Nash and Qiang Zhang Cryst. Growth Des. 2018, 18 (10), pp 6197–6203.

LUMINESCENT MOFS

Luminescent MOFs are usually constructed using luminescent organic ligands and redox innocent metals, such as Zn^{2+}. Cd^{2+}, Al^{3+} and Zr^{4+}. Tetraphenylethene (TPE) based ligands are the ideal candidates for the construction of luminescent MOFs as these ligands are highly emissive at solid state. They possess a very unique property called aggregation induced emission, where the solution of the compound is not emissive, but the solids are highly emissive. As shown in Figure 1.

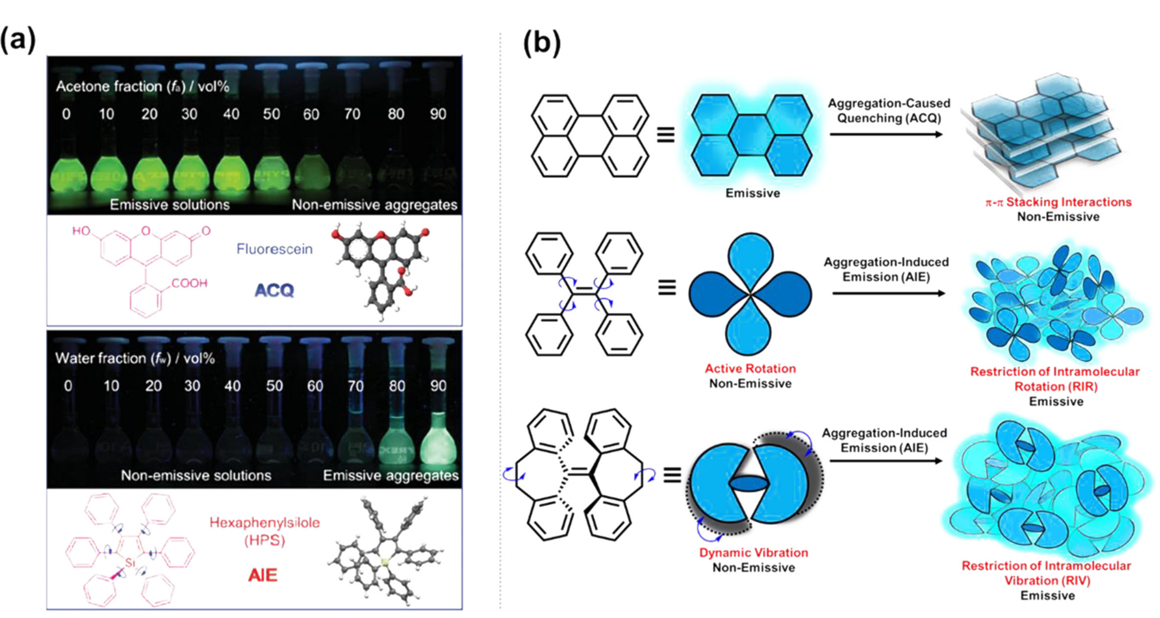

Figure 1. a) Photographs showing the ACQ behavior of fluorescein and AIE properties of HPS, in the mixture of water-miscible organic solvent and water. (b) Schematics showing the general mechanism of ACQ and AIE.

We have used an extended TPE based ligand to react with zirconium cluster to produce a new porous structure, named WSU-5. Interestingly, liner linkers could be inserted into WSU-5 to yield WSU-6 and 7. The insertion of linkers not only changed the structure but also altered the emission of the material.

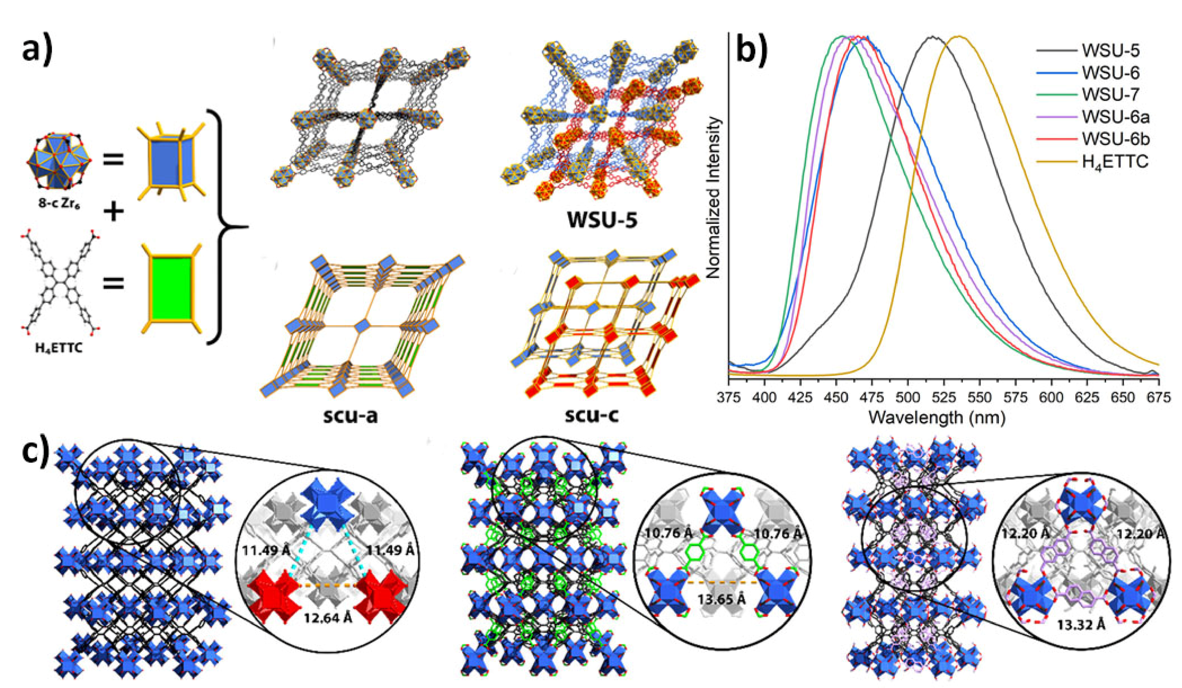

Figure 2. Photoluminescence spectra of WSU-5 (black), WSU-6 (blue), WSU-7 (green), WSU-6a (purple), WSU-6b (red), and H4ETTC (gold) at an excitation wavelength of λ = 350 nm. (c) Illustration of the changes in SBU distances in (a) WSU-5 (b) WSU-6, and (c) WSU-7. Blue and red polyhedra represent Zr6 SBUs of the individual nets of WSU-5.

In another work, we decreased the symmetry of the ligand by removing the carboxylate groups from the para-position to the meta position. The reaction of the new ligand (m-ETTC) with cadmium produced a new structure, named WSU-30. Interestingly, when bipyridine was added, a new porous, mixed-linker MOF was obtained. WSU-31. The change of the structure influenced the luminescence of the material as well. The two materials show different responses when immerged into common solvents.

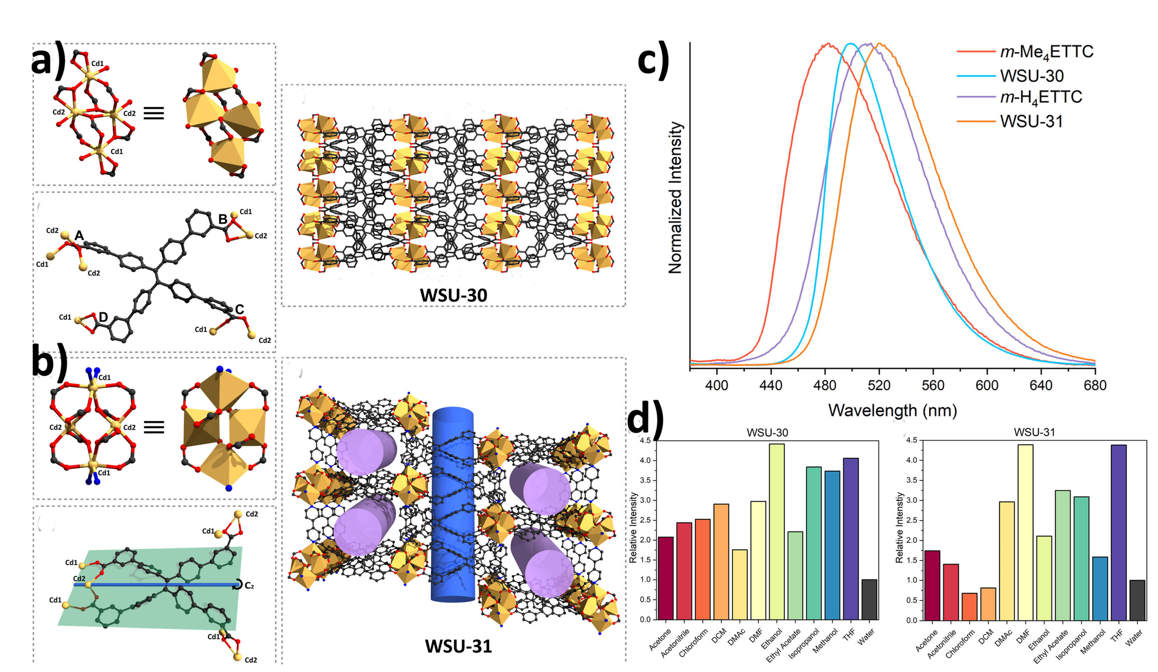

Figure 3. (a) Illustration of the structure of WSU-30. (b) Illustration of the structure of WSU-31. (c) Solid state emissions of m-Me4ETTC (red, λ_{em} = 482 nm), WSU-30 (blue, λ_{em} = 500 nm), m-H4ETTC (purple, λ_{em} =510 nm), and WSU-31 (orange, λ_{em} = 520 nm). (d)Comparison of fluorescent emission intestines in various solvents relative to the emission in water for (a) WSU-30 and (b) WSU-31.

HIERARCHICALLY POROUS MATERIALS FOR CATALYSIS

Most of the reported MOFs possess micropores. It is very expensive and time consuming to enlarge the pores of MOFs as it requires the synthesis of larger organic ligands. In the effort to prepare mesoporous materials with low cost, we have developed a facile method to produce MOF materials based on a microporous material. The synthesis of the microporous MOF, called UiO-66, was modulated so that the small nanocrystals would aggregate and interconnected to form larger particles which possess assorted pores, called hierarchically porous HP-UiO-66. The material demonstrated very high activity in the acetylation reaction of furfural.

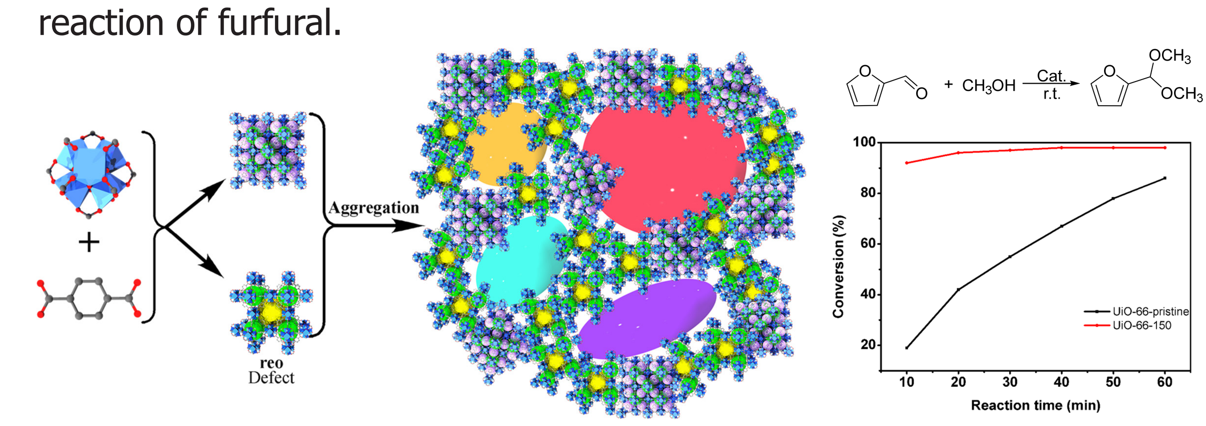

Figure 4. Photographs showing the aggregation of the nanocrystals to form the hierarchically porous material (left). The acetylation reaction of furfural (top right), and the comparison of the catalytic activity of the HP-UiO-66 material with the microporous material (bottom right).

The HP-UiO-66 also show very high activity in the oxidative desulfurization of fuel. Most of the reported catalysts require higher temperature (60 °C) for the desulfurization to work, however, our catalyst could oxidize dibenzothiophene at 30 °C, Figure 5. We have found that our material works better for the oxidative desulfurization owing to the generation of hydroxyl radicals other than superoxide radicals.

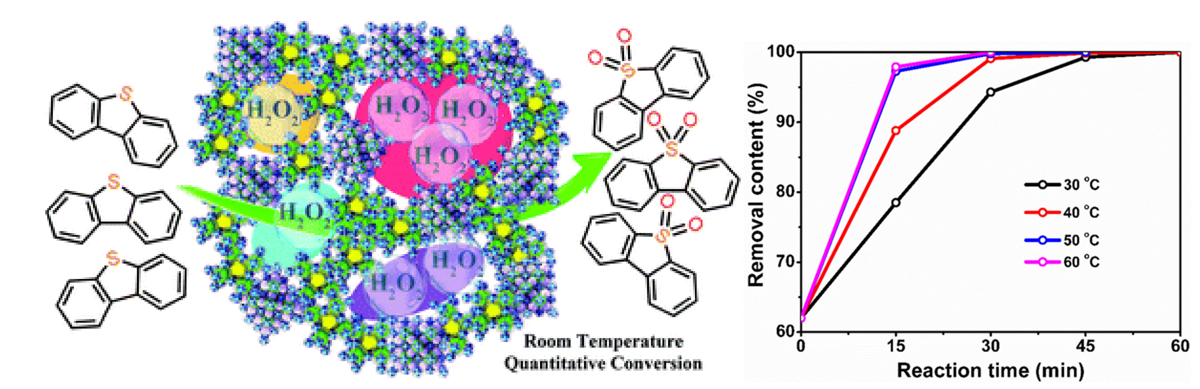

Figure 5 Schematics show the oxidation of dibenzothiophene using HP-UiO-66 and hydrogen peroxide at room temperature (left). The conversion of dibenzothiophene at different temperatures (right).

In another work, we have developed a solvent-free synthesis method to prepare aluminum-based MOFs with phase separations. The combination of benzene tricarboxylate (BTC) and aluminum usually result in three phases, MIL-96 , MIL-100 and MIL-110. The pure phase synthesis requires very specific conditions, such as a narrow pH range and high temperature. What's more, the synthesis often require the use of HF. To develop facile synthesis method for the preparation of Al-BTC MOFs, we have tried several solvent-free reaction conditions, as shown in Figure 6.

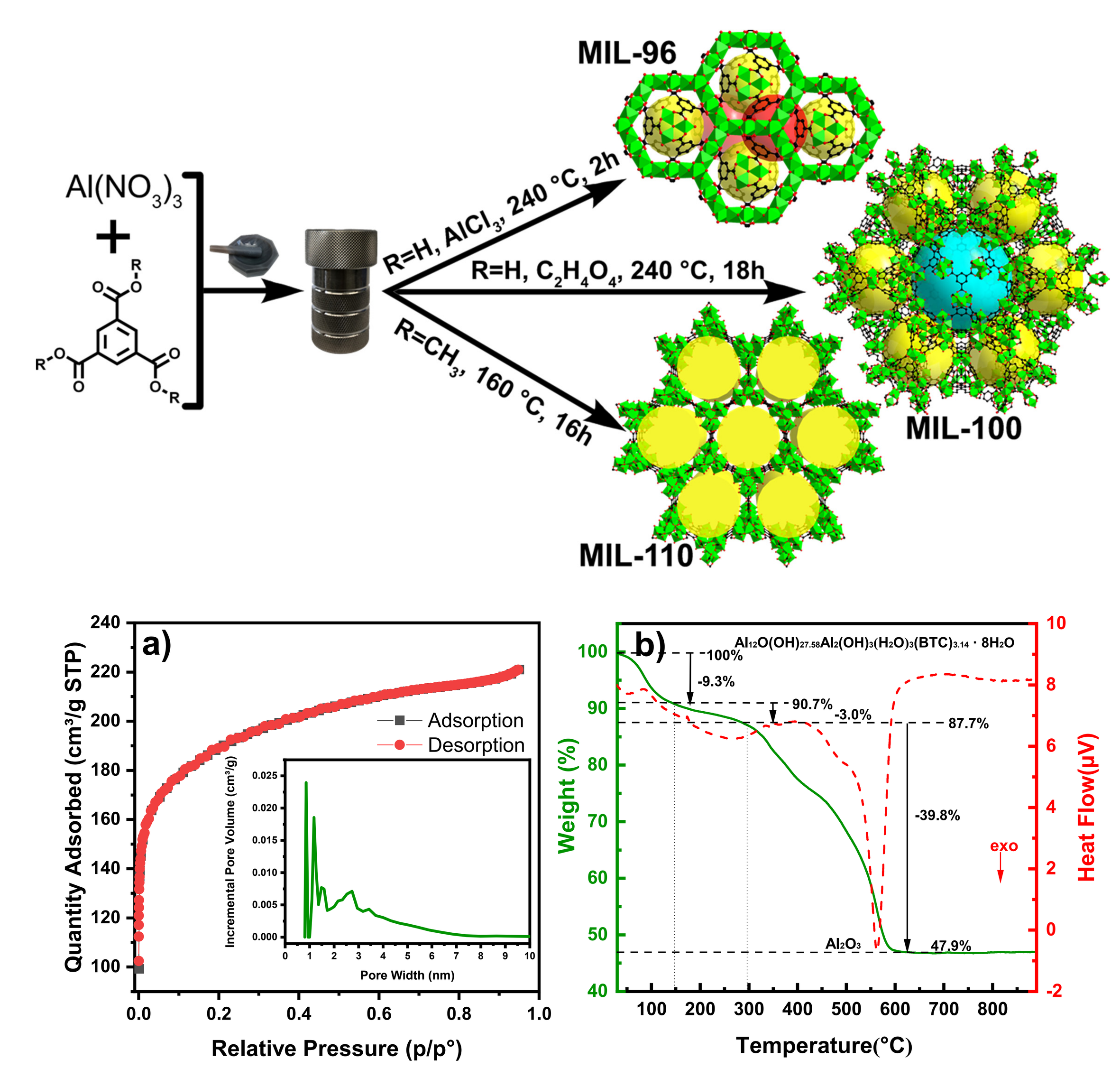

Figure 6. Schematics show the synthesis of Al-BTC MOFs with pure phases under solvent-free conditions (top). The gas adsorption shows the synthesized MIL-96 possesses mesopores (bottom a), and the TGA shows that there are defects in the structure as well (bottom b).

SINGLE-ATOM CATALYSIS

Single-atom catalyst, also called atomically dispersed catalyst, possesses very high catalytic activity compared to nanomaterials and bulk materials. This is because the surface energy increases when the size of the material decreases, Figure 7 left. It is believed that single-atom catalyst possesses the advantages of enzyme, homogeneous and common heterogeneous catalysts, Figure 7 right.

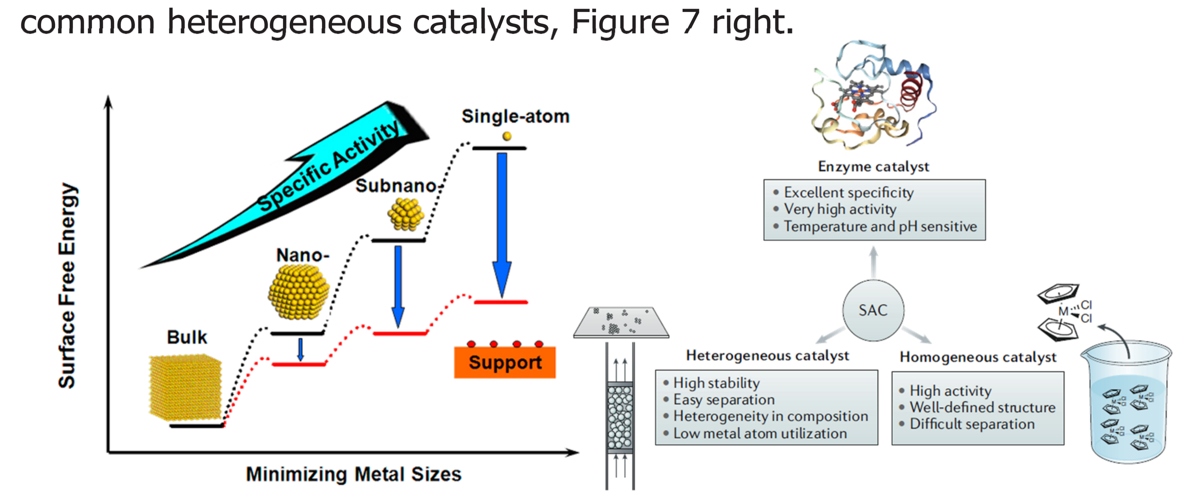

Figure 7. The illustration of surface energy changes upon decreasing the size of the material (left). The single-atom catalyst compares with other types of catalysts (right).

Though single-atom catalyst is superior compared to other catalysts, but the preparation is very tedious, and the scale is very low. In order to synthesis single-atom catalyst easier and in a large scale, we have developed a co-precipitation method, where two metal salts, $Zn(NO_3)_2$ and $ZrO(NO_3)_2$, were used to precipitate under basic conditions. As shown in Figure 8, if the catalyst precursor is added, the resulted material will contain the atomically dispersed metal species.

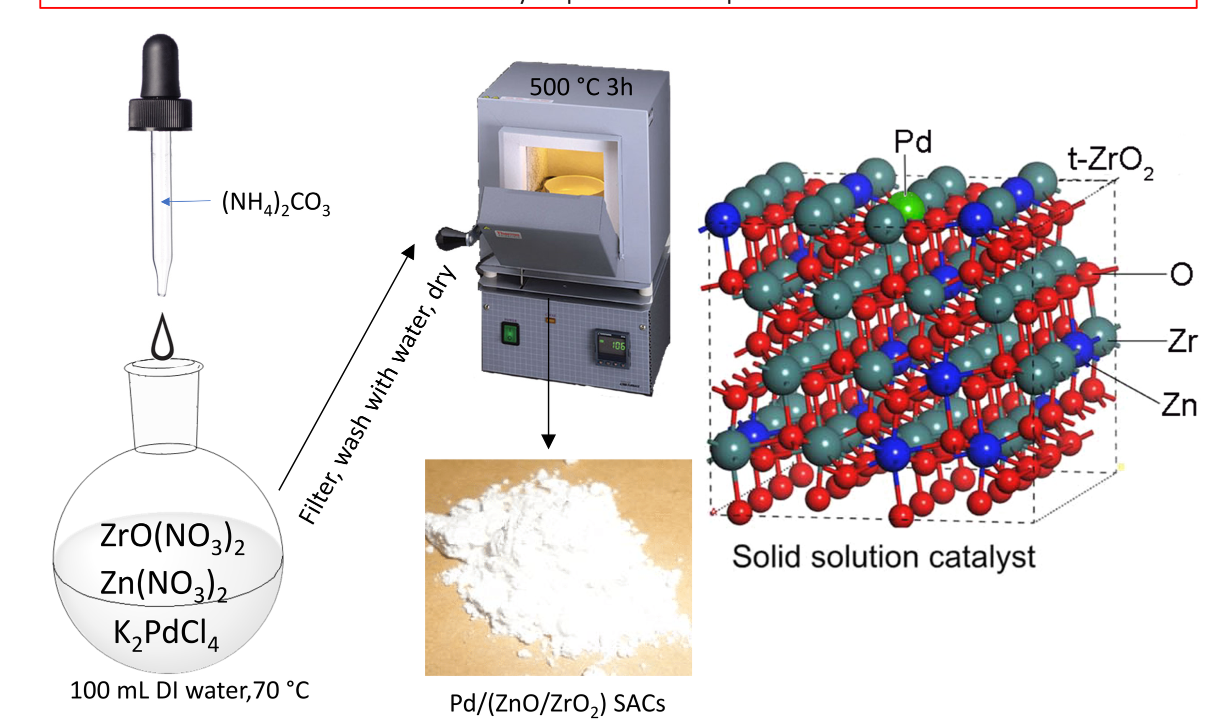

Figure 8. The preparation of the single-atom catalyst using co-precipitation method and heating in a furnace (left). The structure of the prepared single-atom catalyst as a solid solution (right).

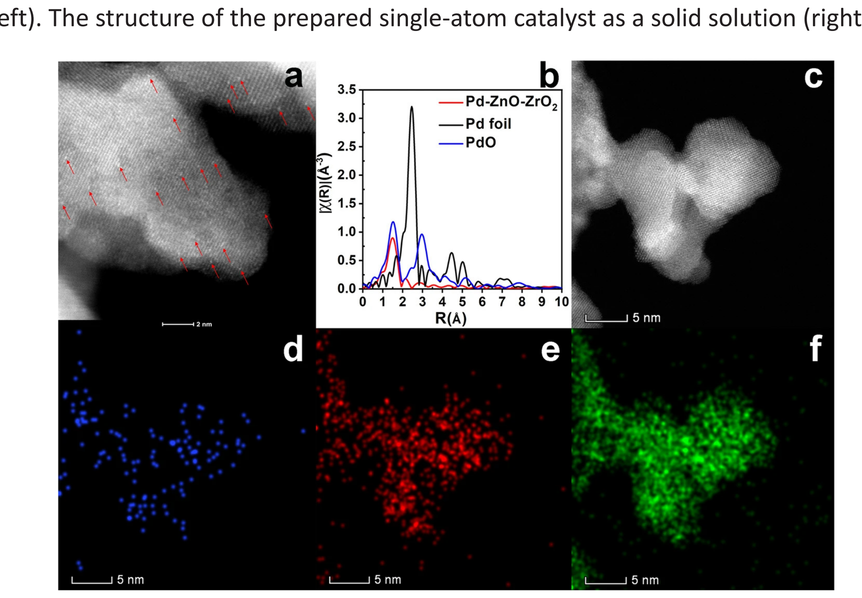

Figure 9. Characterizations showing that the synthesized material does contain atomically dispersed Pd species.

Entry	Aryl Boronic Acid	Aryl Halides	Time/h	Product	Yield/%[a]
1	Me–C_6H_4–B(OH)2	C_6H_5–Br	4	Me–C_6H_4–C_6H_5	93
2	Me–C_6H_4–B(OH)2 (ortho Me)	C_6H_5–Br	7	Me–C_6H_4–C_6H_5 (ortho Me)	93
3[c]	MeO_2C–C_6H_4–B(OH)2	C_6H_5–Br	20	EtO_2C–C_6H_4–C_6H_5	68
4[c]	MeO_2C–C_6H_4–B(OH)2 (meta MeO_2C)	C_6H_5–Br	11	EtO_2C–C_6H_4–C_6H_5 (meta EtO_2C)	81
5	Me–C_6H_4–B(OH)2	Br–C_6H_4–C(O)–C_6H_5	5	Me–C_6H_4–C_6H_4–C(O)–C_6H_5	85
6[d]	Me–C_6H_4–B(OH)2	Br–C_6H_4–Br	11	Me–(C_6H_4)3–Me	86
7[d]	Me–C_6H_4–B(OH)2	Br–C_6H_4–C_6H_4–Br	30	Me–(C_6H_4)4–Me	69
8	C_6H_5–B(OH)2	C_6H_5–I	2	C_6H_5–C_6H_5	93
9	Me–C_6H_4–B(OH)2	I–C_6H_4–OMe	4	Me–C_6H_4–C_6H_4–OMe	93
10	Me–C_6H_4–B(OH)2 (ortho Me)	I–C_6H_4–OMe	4	Me–C_6H_4–C_6H_4–OMe (ortho Me)	87
11[c]	OHC–C_6H_4–B(OH)2	I–C_6H_4–OMe	3	OHC–C_6H_4–C_6H_4–OMe	89
12[d,e]	MeO_2C–C_6H_4–B(OH)2	I–C_6H_4–OMe	3.5	MeO_2C–C_6H_4–C_6H_4–OMe	76
13[d,e]	MeO_2C–C_6H_4–B(OH)2 (meta MeO_2C)	I–C_6H_4–OMe	1.5	MeO_2C–C_6H_4–C_6H_4–OMe (meta MeO_2C)	82
14	C_6H_5–B(OH)2	I–C_6H_4–OMe	7	C_6H_5–C_6H_4–OMe	99
15[d]	Me–C_6H_4–B(OH)2	Me–$C_6H_2(Me)_2$–I	1.5	Me–C_6H_4–$C_6H_2(Me)_2$–Me	88

Table 1. The yield of Suzuki reactions catalyzed by the single-atom Pd catalyst.